Journal of ELECTRONIC MATERIALS, Vol. 48, No. 8, 2019
https://doi.org/10.1007/s11664-019-07343-y
© 2019 The Minerals, Metals & Materials Society

Electrochemical Synthesis of Flower-Like Gold Nanoparticles for SERS Application

NGAN TRUC-QUYNH LUONG ,[1,6] DAO TRAN CAO,[1,2] CAO TUAN ANH,[3] KIEU NGOC MINH,[2] NGUYEN NGOC HAI,[4] and LE VAN VU[5]

1.—Institute of Materials Science, Vietnam Academy of Science and Technology, 18 Hoang Quoc Viet, Hanoi, Vietnam. 2.—Graduate University of Science and Technology, Vietnam Academy of Science and Technology, 18 Hoang Quoc Viet, Hanoi, Vietnam. 3.—Tan Trao University, Trung Mon Commune, Yen Son District, Tuyen Quang Province, Vietnam. 4.—Quang Ninh Department of Education and Training, Halong, Quang Ninh, Vietnam. 5.—University of Science, 334 Nguyen Trai, Thanh Xuan, Hanoi, Vietnam. 6.—e-mail: nganltq@ims.vast.ac.vn

Surface-enhanced Raman spectroscopy (SERS) is a technique that is increasingly used in the identification and quantification of organic molecules at very low concentrations. In this analytical technique SERS-active substrates play a crucial role. Beside silver, gold is also widely used as a material for making SERS substrates. In this report we present a simple method for synthesizing arrays of flower-like gold nanoparticles (also referred to as gold nanoflowers—AuNFs), which can be used as SERS substrates. The AuNFs have been electrodeposited on a silicon surface coated with silver nanoparticles, which served as seeds for the growth of AuNFs. As a result, AuNFs were formed on the silicon surface with relatively dense density and with fairly uniform distribution. Arrays of AuNFs, as SERS substrates, were tested with a rhodamine B (RhB) molecular probe. The results showed that these AuNFs allow the detection of RhB down to a concentration of 1 ppb, a relatively low concentration. This demonstrates the applicability of fabricated AuNFs as a highly active SERS substrate.

Key words: Gold nanoflowers, electrodeposition, surface-enhanced Raman spectroscopy, rhodamine B

INTRODUCTION

At present, surface-enhanced Raman scattering (SERS) is increasingly being used as a method for detecting traces of contaminants in a variety of specimens. In order to maximize SERS's performance, the most important thing is to have highly active SERS substrates. Highly active SERS substrates are substrates capable of boosting the Raman scattering signal to several orders. In turn, this depends on how many "hot spots" there are in the substrate, i.e,. the areas in which the great enhancement of the electromagnetic field exists. Normally, hot spots appear around the sharp edges or corners of the metal surface, or in the small gap (less than 10 nm) between the two metal surfaces.[1] To get more sharp points, there have been many attempts to design SERS substrates not in the form of aggregates of spherical metal nanoparticles but as a set of branched nanoparticles. Flower-like metallic nanoparticles (also referred to as metallic nanoflowers) are a typical branched nanostructure, so they are prioritized to be used as SERS substrates. For example, while using different shape gold nanostructures (nanowire networks, nanosheets, and nanoflower arrays on the solid substrates) as SERS subtrates for detecting traces of 4-aminothiophenol (4-ATP), Wang et al.[2] have found that the nanoflower array films give the largest enhancement factor. Note that although it is widely known that silver has the greatest Raman enhancement potential when used as a SERS

(Received February 3, 2019; accepted June 1, 2019; published online June 11, 2019)

substrate, gold has a number of advantages, such as sustainibility for oxidation as well as good biological compatibility, therefore it is also used as a substrate for SERS in many cases.

There are numerous reports in the literature on the synthesis of gold nanoflowers (AuNFs) for use as SERS substrates.[2–22] Among them, a large number of the articles reported the results of AuNF colloidal suspension synthesis,[3–16] only a few papers presented the results of the fabrication of AuNF arrays on solid substrates.[2,17–22] In order to synthesize AuNFs, the seed-mediated approach has been used by a number of research groups,[5,14,16,18,21] because this approach has the advantage of separating the stages of nucleation and growth of nanoflowers, and thus a better control over the size, size distribution and shape evolution of nanoflowers is provided. However, it should be noted that so far the reports in the literature have used only gold nanoparticles to germinate the growth of AuNFs.

In this report we will present a way to synthesize an array of AuNFs on silicon for use as SERS substrates and then provide an illustration of the effectiveness of this substrate. Our way of synthesizing AuNFs is special compared to those of published papers in the following points. First of all, there are currently two main types of SERS substrates, namely the colloidal solution of metallic (mainly silver or gold) nanoparticles and the array of metallic nanoparticles immobilized on a certain solid substrate. We chose to make the second type of substrates to avoid the agitation of the nanoparticles in the colloidal solution, which affects the stability and reproducibility of the Raman signal. Secondly, like many other research groups, we have chosen the seed-mediated growth to making AuNFs, however we have used silver nanoparticles as seed instead of gold nanoparticles. The advantage of this approach is that silver promotes the anisotropic growth of gold nanoparticles on some specific crystal axes, so that the flower structure is formed more easily, as recently reported in the review of Ujihara.[23] Thirdly, we used electrochemical deposition in both stages of the AuNFs synthesis process, nucleation and growth. In the literature, the number of reports using electrochemical methods to synthesize AuNFs is very limited.[20–22] Meanwhile, in our opinion, the combination of the two factors, namely the electric element and the chemical element in the electrochemical deposition, will make the synthesis process much better controlled.

EXPERIMENTAL

The initial silicon used was a single crystalline silicon (Si) wafer, crystal orientation (100) and resistivity 0.1–10 Ω cm. First, Si wafers were washed in absolute ethanol (5 min), acetone (5 min), HNO_3/H_2O = 1/1 (10 min), 5% HF (5 min) and deionized water (several times). Then a thin layer of aluminum was deposited on the backside of the Si wafer by vacuum evaporation (this aluminum layer is used to create the ohmic contact). The next step is to cut the Si wafer into samples of 0.6×0.6 cm^2 and perform an electrodeposition process to produce an array of silver nanoparticles (AgNPs) on the silicon surface. Electrodeposition was carried out under the constant current mode with a current density of 0.05 mA/cm^2 for 3 min at room temperature in an aqueous solution of $AgNO_3$ (0.1 mM) and HF (0.14 M). The electrochemical system consists of two electrodes, with the Al-coated Si sample serving as a cathode, while a platinum grid is the anode. Once created, AgNPs will be used as seeds for the growth of AuNFs. The electrodeposition of AuNFs was performed in a similar way to the electrodeposition of AgNPs, except that it was caried out at a current density of 0.1 mA/cm^2 for 10 min in an aqueous solution containing 0.1 mM $HAuCl_4$ and 0.14 M HF. After fabrication, the samples with AuNFs grown on silicon (AuNFs@Si) were washed with deionized water several times and dried in air.

The surface morphology of the AuNFs@Si samples was investigated using the S-4800 field effect scanning electron microscope (Hitachi, Japan). X-ray diffraction measurements have also been performed on several representative samples to check whether the obtained nanoflowers are crystallized gold. This measurement was performed on a Bruker-AXS D5005 x-ray diffraction system (Siemens, Germany). SERS measurements were performed by dripping 25 μl of aqueous RhB at various concentrations on the AuNFs@Si substrate. The samples were then allowed to dry naturally in air at room temperature. The Raman spectra of the samples were recorded by a portable i-RamanPro spectrometer (model BWS475-785H produced by B&W Tek, Inc., USA) with a 785 nm excitation laser. The full laser power at the probe excitation position is 427 mW and the laser spot size is 105 μm (for the objective lens magnification of 20 ×). This spectrometer provides a Raman spectrum over the range of 65–2800 cm^{-1} with a spectral resolution of better than 3.5 cm^{-1}.

RESULTS AND DISCUSSION

First, by electrodeposition, we tried to make AuNFs on silicon substrates without seed. However, this work was unsuccessful, although different fabrication conditions were used. The results were always just gold nano-grains with irregular shapes. So we switched to the seed-mediated growth of AuNFs. We used silver nanoparticles (AgNPs) as seeds for growing AuNFs. The reason for this is that some reports in the literature, especially the recent review of Ujihara, have shown that silver seed is particularly suitable for the growth of branched gold structures.[23] More specifically, it has been found that silver will promote anisotropic growth of gold nanocrystals on certain crystal axes. This means

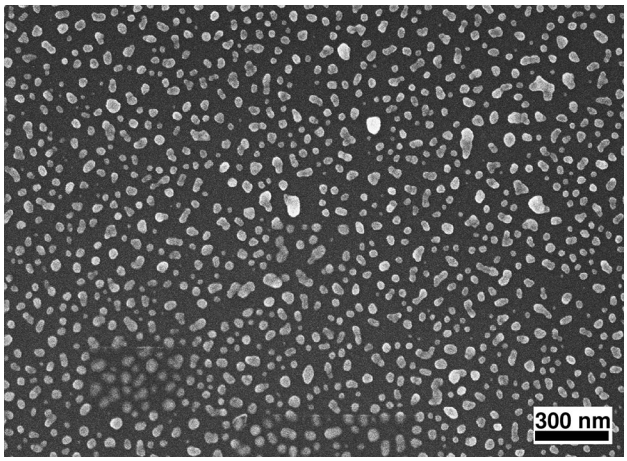

Fig. 1. Plane-view SEM image of AgNPs obtained by electrodeposition with 0.05 mA/cm^2 constant current for 3 min in the solution containing 0.1 mM $AgNO_3$ and 0.14 M HF on the silicon substrate.

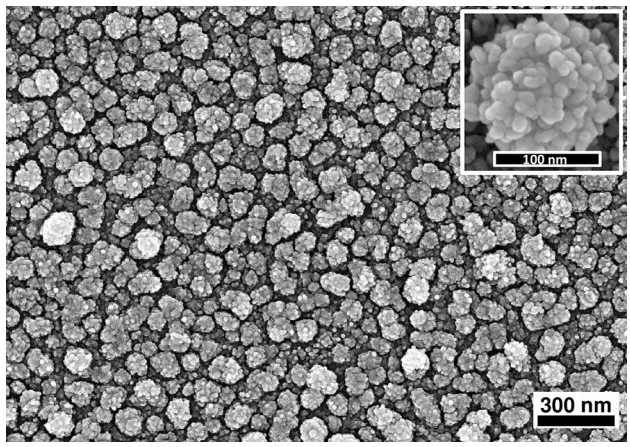

Fig. 2. Plane-view SEM image of AuNFs obtained by electrodeposition with 0.1 mA/cm^2 constant current for 10 min in the solution containing 0.1 mM $HAuCl_4$ and 0.14 M HF on the AgNPs-coated silicon substrate.

that the gold nano-flower structure will form more easily. Although AgNPs have not previously been used as seeds, it is remarkable that many authors have emphasized the role of silver ions in particular and foreign ions in general, in the seed-mediated growth of gold nanostructures with different shapes (nanorods, nanostars…).[24–27] In this study, the synthesis of AgNPs (for use as seeds in the next step) was also performed by electrodeposition. The synthesis conditions are derived from our previous works.[28,29] Silver electrodeposition under constant current mode with different current densities was used. The results show that the optimal AgNP array is obtained when the current density is 0.05 mA/cm^2. This array is illustrated in Fig. 1. From Fig. 1 we can see that AgNPs are nearly spherical or elongated particles, with an average size of about 40 nm, the distance between AgNPs is about hundreds of nm. Once we had the silver seeds, we proceeded to grow from them the gold nanoflowers. The growth was carried out by electrodeposition in an aqueous solution of gold salt ($HAuCl_4$) and HF in constant current mode. The different current densities were used and it was found that the current density of 0.1 mA/cm^2 gives the best results. The array of AuNFs fabricated under such conditions is illustrated in Fig. 2. Figure 2 shows that the gold flowers are fairly uniform in size in the 100–200 nm range, with an average size of 130 nm. The flower density is quite high with about 20 nm average distance between flowers. In addition, each gold flower has a large number (several dozen) of petals. To test whether the flowers obtained were actually gold or not, and in what form, we conducted x-ray diffraction (XRD) measurements. The XRD spectrum of a representative AuNFs array is shown in Fig. 3. The results show that AuNFs are formed in crystalline form. More specifically, the XRD spectrum shows peaks at 2θ diffraction angles equal to

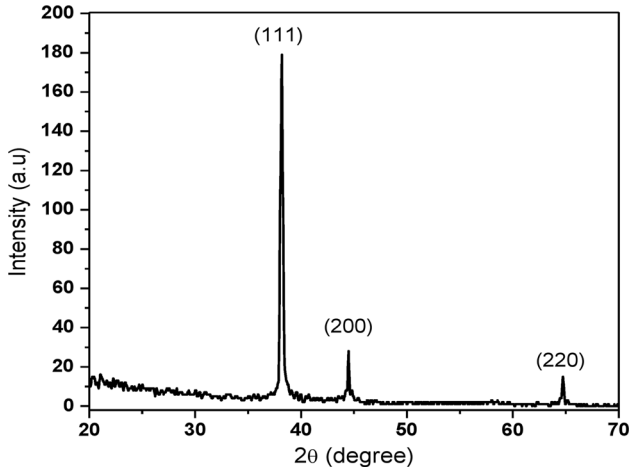

Fig. 3. X-ray diffraction spectrum of an AuNFs array obtained by electrodeposition with 0.1 mA/cm^2 constant current for 10 min in the solution containing 0.1 mM $HAuCl_4$ and 0.14 M HF.

38.2°, 44.5° and 64.7° corresponding to the plane families (111), (200) and (220) of Au crystal with the face centered cubic (FCC) structure.[30,31]

With the above morphology and arrangement of AuNFs, we believe that the AuNF arrays synthesized under optimal conditions can serve as highly active SERS substrates. Indeed, when using such AuNF arrays as the SERS substrates to record the Raman spectra of rhodamine B (RhB) molecules, we obtained spectra with clearly distinct RhB peaks in the concentration range of 5 ppm to 0.1 ppb as shown in Fig. 4. The correspondence between Raman bands and vibration modes is as follows.[32] The peak located at 619 cm^{-1} is assigned to the xanthene ring puckering mode. The bands in the region of 1100–1700 cm^{-1} on the SERS spectra of RhB are related to C–C bridge band stretching and aromatic (1196 cm^{-1}), C–H bending vibration

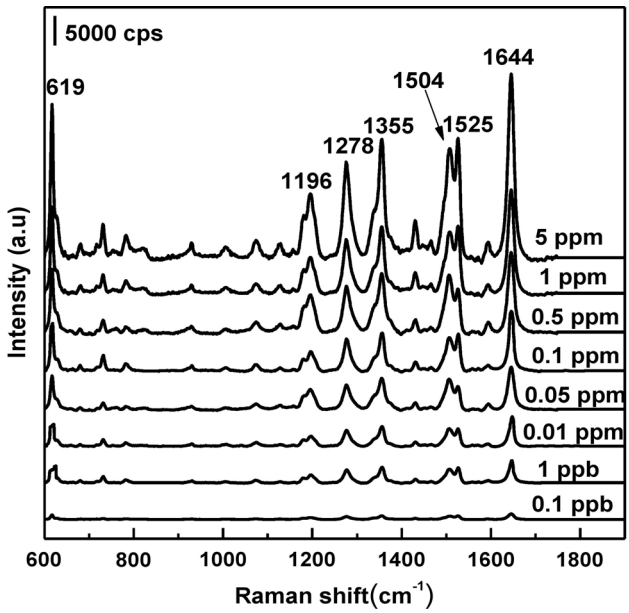

Fig. 4. SERS spectra of rhodamine B (RhB) at different concentrations in the region from 5 ppm to 0.1 ppb, which have been recorded using the identical AuNFs@Si arrays electrodeposited at 0.1 mA/cm^2 constant current as SERS substrates.

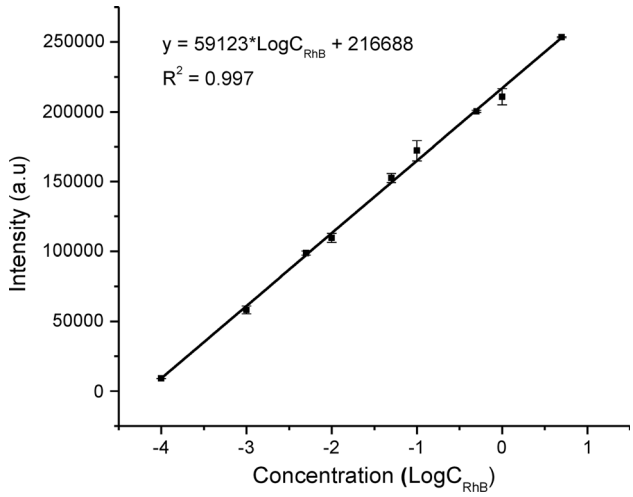

Fig. 5. The functional relationship between Raman intensity of the peak at 1644 cm^{-1} and RhB concentration. The error bars are standard deviations from a total of three measurements.

(1278 cm^{-1}), aromatic C–C bending and C=C stretching (1355 cm^{-1} and 1644 cm^{-1}), and aromatic C–H bending (1504 cm^{-1} and 1526 cm^{-1}). It is well known that RhB is an organic dye commonly used to test the activity of SERS substrates. In addition, it is a colorant used in the paper, textile and ceramics industries. When absorbed into the body, RhB can mutate and cause cancer to humans as well as animals.[33] Consequently, the use of this dye in food processing is prohibited. However, at present in a series of countries it is still illegally used in food processing to produce bright red color.[32] Due to the negative impact of RhB on human health, rapid, sensitive and cost-effective detection of RhB residues in food itself is valuable and necessary.

For quantitative analysis, it is possible to choose the peak located at 1644 cm^{-1} to represent RhB. This is a single peak, furthermore it has the greatest intensity in the SERS spectrum of RhB. The functional relationship between SERS intensity of the 1644 cm^{-1} peak and the RhB concentration is plotted in Fig. 5. In this figure we can see a good linear relationship between the SERS intensity and the RhB concentration in the region from 0.1 ppb to 5 ppm. The regression equation is $y = 59123\text{Log}C_{\text{RhB}} + 216688$ and $R^2 = 0.997$, where y is the SERS intensities of the peak at 1644 cm^{-1} of RhB, and C_{RhB} represents RhB concentration. Note that each point in Fig. 5 is the result of averaging the three measurements at different points on the same sample. The error bars represent the standard deviations of three independent measurements. The limit of detection (LOD) of RhB was 0.01 ppb, estimated by the signal-to-noise ratio of 3 ($S/N = 3$). This result shows that the SERS substrates made from AuNFs synthesized according to the method we have presented can be used for rapid and accurate quantitative analysis of RhB.

CONCLUSIONS

By electrodeposition combined with the use of silver nanoparticles as seeds, we have successfully fabricated arrays of gold nanoflowers on silicon (AuNFs@Si). The gold nanoflowers have quite a lot of petals, and they are fairly uniform throughout the array with an average size of about 130 nm. Reproducibility of nanoflowers for different production times is quite good. Arrays of AuNFs@Si have demonstrated the ability to work as highly active SERS substrates. Specifically, Raman spectral results with the Rhodamine B (RhB) probe have shown that these SERS substrates allow detection of RhB with the detection limit of 0.01 ppb. The good linear relationship ($R^2 = 0.997$) between the SERS intensity and the RhB concentration in the range of 0.1 ppb to 5 ppm demonstrates that the AuNFs@Si substrates can serve well for the purpose of RhB's trace analysis.

ACKNOWLEDGMENTS

This work was supported financially by the Ministry of Science and Technology of Vietnam under Project 01/2018/DTDL.CN-XNT.

REFERENCES

1. H. Tang, C. Zhu, G. Meng, and N. Wu, *J. Electrochem. Soc.* 165, B3098 (2018).
2. T. Wang, X. Hu, and S. Dong, *J. Phys. Chem. B* 110, 16930 (2006).

3. B.K. Jena and C.R. Raj, *Langmuir* 23, 4064 (2007).
4. B.K. Jena and C.R. Raj, *Chem. Mater.* 20, 3546 (2008).
5. L. Zhao, X. Ji, X. Sun, J. Li, W. Yang, and X. Peng, *J. Phys. Chem. C* 113, 16645 (2009).
6. S. Boca, D. Rugina, A. Pintea, L. Barbu-Tudoran, and S. Astilean, *Nanotechnology* 22, 055702 (2011).
7. Y. Jiang, X.-J. Wu, Q. Li, J. Li, and D. Xu, *Nanotechnology* 22, 385601 (2011).
8. Y. Ren, C. Xu, M. Wu, M. Niu, and Y. Fang, *Colloids Surf. A* 380, 222 (2011).
9. M. Pradhan, J. Chowdhury, S. Sarkar, A.K. Sinha, and T. Pal, *J. Phys. Chem. C* 116, 24301 (2012).
10. S. Yi, L. Sun, S.C. Lenaghan, Y. Wang, X. Chong, Z. Zhang, and M. Zhang, *RSC Adv.* 3, 10139 (2013).
11. J. Yoo and S.-W. Lee, *Bull. Korean Chem. Soc.* 35, 2765 (2014).
12. F.A. Mahyari, M. Tohidi, and A. Safavi, *Mater. Res. Express* 3, 095006 (2016).
13. C. Song, B. Yang, W. Chen, Y. Dou, Y. Yang, N. Zhou, and L. Wang, *J. Mater. Chem. B* 4, 7112 (2016).
14. S. Zhen, T. Wu, X. Huang, Y. Li, and C. Huang, *Sci China Chem.* 59, 1045 (2016).
15. D.-P. Yang, X. Liu, C.P. Teng, C. Owh, K.Y. Win, M. Lin, X.J. Loh, Y.-L. Wu, Z. Li, and E. Ye, *Nanoscale* 9, 15753 (2017).
16. F. Liebig, R. Henning, R.M. Sarhan, C. Prietzel, M. Bargheer, and J. Koetz, *Nanotechnology* 29, 185603 (2018).
17. J.N. Krishnan, I.T. Kim, S.-H. Ahn, Z.H. Kim, and S.K. Kim, *ECS Trans.* 25, 81 (2009).
18. A.K. Das and C.R. Raj, *J. Electroanal. Chem.* 638, 189 (2010).
19. K. Winkler, A. Kaminska, T. Wojciechowski, R. Holyst, and M. Fialkowski, *Plasmonics* 6, 697 (2011).
20. G. Duan, W. Cai, Y. Luo, Z. Li, and Y. Li, *Appl. Phys. Lett.* 89, 211905 (2006).
21. J.-H. Kim, T. Kang, S.M. Yoo, S.Y. Lee, B. Kim, and Y.-K. Choi, *Nanotechnology* 20, 235302 (2009).
22. Y. Bu and S.-W. Lee, *Microchim. Acta* 182, 1313 (2015).
23. M. Ujihara, *J. Oleo Sci.* 67, 689 (2018).
24. N.R. Jana, L. Gearheart, and C.J. Murphy, *Adv. Mater.* 13, 1389 (2001).
25. M. Grzelczak, J. Perez-Juste, P. Mulvaney, and L.M. Liz-Marzan, *Chem. Soc. Rev.* 37, 1783 (2008).
26. H.J. Wang, C.Y. Xue, R. Chen, and W.D. Zhang, *Adv. Mater. Res.* 152–153, 600 (2011).
27. J.G. Wang, X.W. Cao, L. Li, T. Li, and R. Wang, *J. Phys. Chem. C* 117, 15817 (2013).
28. T.C. Dao, T.Q.N. Luong, T.A. Cao, N.H. Nguyen, N.M. Kieu, T.T. Luong, and V.V. Le, *Adv. Nat. Sci.: Nanosci. Nanotechnol.* 6, 035012 (2015).
29. T.C. Dao, N.M. Kieu, T.Q.L. Luong, T.A. Cao, N.H. Nguyen, and V.V. Le, *Adv. Nat. Sci.: Nanosci. Nanotechnol.* 9, 025006 (2018).
30. V.G. Praig, G. Piret, M. Manesse, X. Castel, R. Boukherroub, and S. Szunerits, *Electrochim. Acta* 53, 7838 (2008).
31. J. Elias, M. Gizowska, P. Brodard, R. Widmer, Y. Hazan, T. Graule, J. Michler, and L. Philippe, *Nanotechnology* 23, 255705 (2012).
32. S. Lin, W. Hasi, X. Lin, S. Han, X. Lou, F. Yang, D. Lin, and Z. Lu, *Anal. Methods* 7, 5289 (2015).
33. H. Zhang, J. Wang, H. Wang, and X. Tian, *Mater. Res. Express* 4, 095009 (2017).

Publisher's Note Springer Nature remains neutral with regard to jurisdictional claims in published maps and institutional affiliations.